Lecture

Progress in Quantitative Sputter Depth Profiling using the MRI- model

Siegfried Hofmann and Jiang Yong Wang
Max-Planck-Institute for Metals Research
Heisenbergstr.3
70569 Stuttgart, Germany
s.hofmann@mf.mpg.de

(Received: Jan. 16, 2003)

Recent applications and future prospects show the progress in quantitative sputter depth profiling using the MRI model. Examples are prediction of the influence of backside depth profiling in SIMS, estimation of the sputtered depth in AES depth profiles by using the shift between high and low energy Auger peak measurement, and quantitative determination of the diffusivity in nanostructures. Nonlinear concentration/intensity and depth/time relations caused by preferential sputtering of a component can be taken into account, and further modifications by introducing composition dependent mixing length and information depth parameters will lead to an improved accuracy in profile reconstruction.

1. Introduction

Quantitative depth profiling is relatively easy when the depth resolution is small against the shape of the profile we want to disclose. In that case, and if the usual dependence of the sputtering rate on composition ("preferential sputtering") is negligible, we only need to quantify the intensity scale in an elemental concentration scale, and the sputtering time scale in a depth scale. Of course, the latter is only straight forward if. However, if the above conditions are not met, we have to quantify by using deconvolution or profile reconstruction methods to get the true in depth distribution of composition.[1]. That means we have to know not only the depth resolution, but the depth resolution function. An adequate description of the depth resolution function is possible with the MRI-model, that is described in more detail in several review articles [1,2,3]. The MRI-model is based on the three fundamental parameters in sputter depth profiling, atomic mixing (M), roughness (R), and information depth (I). Since we use the profile reconstruction method by "forward" calculation of the convolution integral [1], we can approach the true in depth distribution by taking into account nonlinear effects [2]. The simple MRI-model has already shown its usefulness in many applications [4,5], and a user-friendly version is available in the COMPRO software of the SASJ. In the following, we will focus on recent progress in specific applications and on some modifications of the MRI parameters that will result in higher accuracy of profile quantification.

2. Asymmetry of the depth resolution function: Backside profiling

When the influence of roughness is sufficiently small, the depth resolution function in SIMS (where we can most often neglect the information depth parameter) is governed by the mixing length. That means, it is usually rather asymmetric: with a steep increase in front and an exponentially decaying trailing edge[6]. Therefore, a steep rise in a depth distribution is much better represented in the measured profile than a steep decrease. When sputter depth profiling is performed from the direction of the backside of the sample, we should obtain a better resolution of the rear part of a depth distribution. However, care has to be taken to suppress roughening during sample thinning from the backside. An excellent example was recently given by K. L. Yeo et al. [7], who succeeded in keeping the roughness low (<0.4 nm) by using a silicon-on-insulator substrate. The Si(100) layer was implanted with 0.5 keV Boron ions and was analyzed with a CAMECA IMS-6f instrument with 0.5-5 keV O_2^+ beams at oblique incidence (44-56 deg.). The B distribution is ideally

Gaussian, but owing to channeling effects the trailing edge can be described by an exponential function with a decay length of 3.7 nm [7]. Fig. 1a shows the MRI calculation result for the case of an in depth distribution of exponentially increasing (simulating backside sputter profiling) and exponentially decreasing (frontside profiling) concentration with a constant concentration of 17 nm in between. Results are shown for 2 and 5 keV O_2^+ ion energies. The mixing length is difficult to estimate, because the probable ion range is more likely to be that of SiO_2, since we are in both cases in the steady state regime of sputtering. Taking the average value (from TRIM ion range) of w = 3.0 and 4.9 nm for 2 and 5 keV, respectively, σ =0.3 nm and λ = 0.3 nm (= about 1 ML adequate for SIMS [1,2]), we obtain the profiles shown in Fig. 1a in logarithmic ordinate scale. It is clearly seen that the "backside" decay length (left side) stays practically constant with ion energy, whereas the "frontside" decay length (right side) considerably increases with energy.

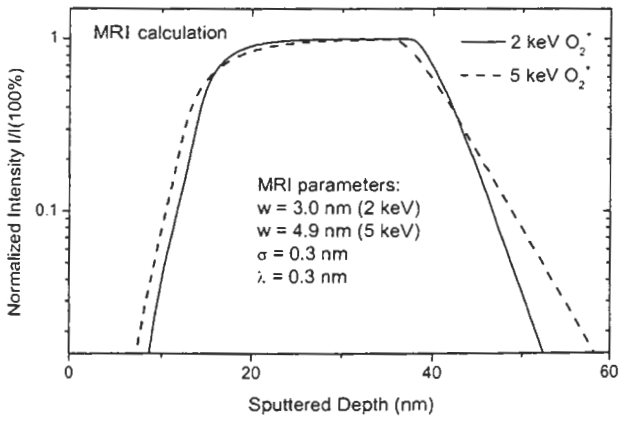

Fig. 1a: MRI calculation for an original distribution characterized by an exponential concentration increase of one decade per 3.7 nm, and after 17 nm at concentration =1, the same exponential decrease, for w parameters taken from TRIM ion ranges of O in SiO_2, simulating usual (front) and backside sputter profiling of an exponentially decaying profile. (The parameters were chosen with respect to [7]).

Fig 1b shows a comparison of the MRI calculated values with the measured values of Yeo et al. [7], without any further fitting. It should be noted, that the mixing length is (a) not very well defined by TRIM ion range, and (b) it is decreased with respect to the Si original matrix scale by "swelling" due to oxide formation by O_2^+ bombardment. The results show that higher energy ions can be used in backside profiling without distorting the original profile. The slight increase for the measured backside case is probably due to the increasing mixing length "straggling" with increasing ion energy [1,2].

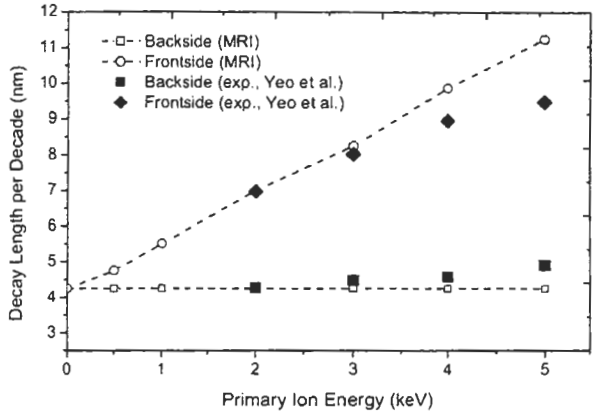

Fig. 1b: Decay length as a function of the primary ion energy for frontside and backside sputtering. Comparison of the results of calculations as depicted in Fig. 1 a with the experimental data of Yeo et al. [7].

3. Profile shift and estimation of the depth scale

As shown earlier [8], according to the MRI model the measured profile is shifted with respect to the original in depth distribution in direction to the surface. This shift depends on the mixing length as well as on the information depth. Because that is different for low and high energy Auger electrons in AES depth profiling, we expect a different shift or a mutual shift on the sputtering time scale if both peaks for one element are recorded simultaneously. That mutual shift, $\Delta z_{sh}(\lambda)$ is directly related to the difference between the respective electron escape depth values, $\lambda_2 - \lambda_1$. In fact, for negligible mixing influence ($w/\lambda<0.69$) the relation $\Delta z_{sh}(\lambda) = 0.7\ (\lambda_2 - \lambda_1)$ is valid. For the 50 % intensity value of an interface profile [8,9]. For higher mixing length ($w/\lambda>0.69$), the relation is more complicated and is given by [8,9]:

$$z_{sh}(\lambda) = -w \times \ln\left[\frac{1-\exp(-w/\lambda_1)}{1-\exp(-w/\lambda_2)}\right] \quad (1)$$

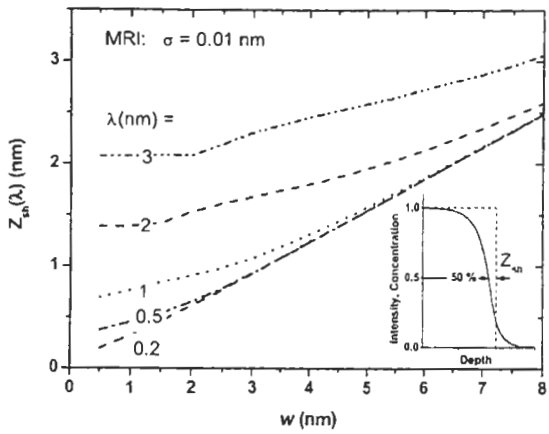

Fig. 2a: Shift of the 50% decay (or increase) value of a measured interface profile as a function of the mixing length w, for different information depth parameters λ and negligible σ.

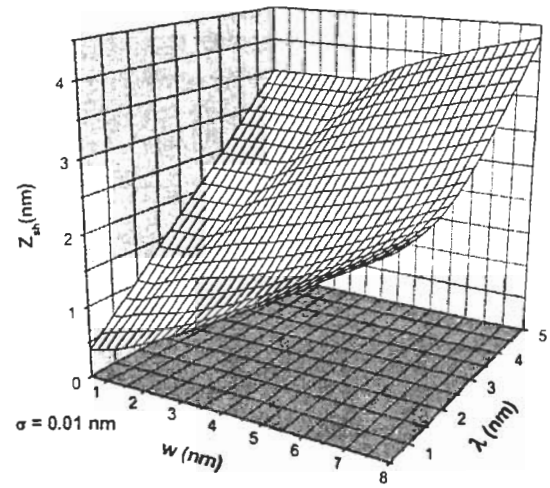

Fig. 2b: Plots as Fig.2a, but in three coordinates.

Fig.2a shows the dependence of the shift of the 50% value of a measured profile at a sharp interface (see inset) against that interface as a function of w for different values of λ. It is clearly recognized, that the largest differences in the shift are obtained for relatively small mixing lengths w. For example, the shift difference between λ_1=0.5 and λ_2= 2 nm decreases from 0.9 nm for w = 1 nm to 0.3 nm for w = 8 nm. Fig. 2b shows the interdependence of z_{sh}, w and λ in a three-dimensional plot.

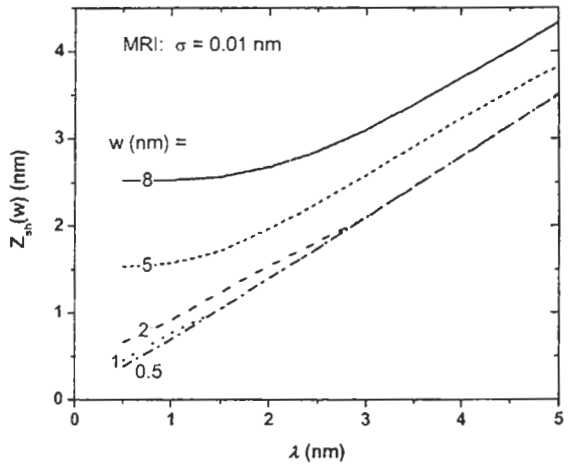

Fig. 2c: Shift of the 50% decay (or increase) value as a function of λ for different w parameters.

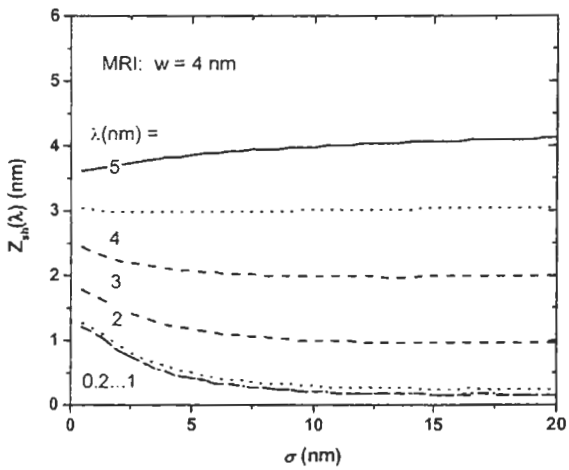

Fig. 2d: Shift of the 50% decay (or increase) value as a function of σ for different λ parameters for w=4 nm.

Fig. 2c depicts the dependence of the shift on λ for different values of w. It is interesting to note that for small values of w (< 2 nm), the shift is almost independent of w, particularly at higher λ values. For higher values of w, the shift is about 0.3 w, and almost independent of λ for λ<< w. Finally, Fig. 2d shows the dependence of the profile shift on the roughness parameter,σ, for different values of λ, with a fixed w = 4 nm. For low values of λ the shift initially decreases with increasing roughness, but for high values of λ the behavior is opposite. Of course, in particular this somewhat strange behavior requires experimental proof, but to the authors' knowledge, there are no experiments for comparison. Only the dependence shown in Figs. 2 a,b has been verified several times

[8,9]. It is of practical importance for the determination of the depth scale in AES depth profiling, because the shift of the measured profiles of the same element with a high and low energy peak (such as Al, Si, Cu, Ni, etc.) show a shift on the time scale that can be directly compared with the above determined shift in nm dimension, the ratio giving the average sputtering rate [9,10].

4. Nonlinear concentration scale: Cluster emission in SIMS

The flexibility of the MRI model allows to take into account matrix effects that result in a nonlinear relation between the measured intensity and the actual surface concentration. Such a nonlinearity was quantitatively determined for the emission of positive ion clusters of Al_2^+ and Al_3^+ in SIMS depth profiling of a double layer structure of Al As in GaAs [12]. Quantification by the MRI model yielded a dependence of the respective ion intensity, I, on the surface concentration, X, of the form I= const. X^n, with the exponent n=1, 1.6, and 2.5, for the ions Al^+, Al_2^+ and Al_3^+, respectively. This demonstrates another important application field of the MRI model.

5. Nonlinear depth scale: Influence of preferential sputtering

Preferential sputtering of a component of the sample is a notoriously difficult problem for quantification, particularly in AES depth profiling. It affects not only the composition of the altered layer (= the mixing zone), but also the instantaneous sputtering rate and therefore leads to a nonlinear sputtered depth/ sputtering time relation in a concentration gradient. Assuming, as a first order approximation, a linear dependence of the sputtering rate on the surface composition, this relation can easily be introduced in the MRI model. As an example, the shape of a Ta/Si multiplayer profile was correctly predicted when a sputtering rate ratio of pure Si to pure Ta of 3.5 was assumed [13]. The calculated and measured profiles for this case are shown in Fig. 3a, with the respective MRI parameters given in the caption. The typical asymmetric shape of the Si profile is a direct consequence of preferential sputtering when atomic mixing is preponderant. For dominating roughness influence, a multilayer profile looks as shown in Fig. 3b. This is valid for the case of a Ni/Cr multilayer sputter depth profiled with N_2^+ ions [14].

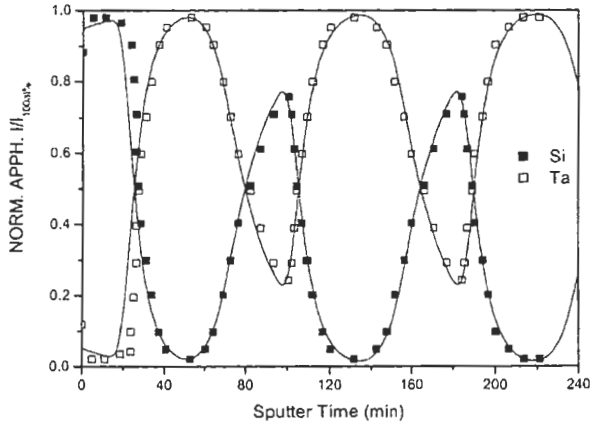

Fig. 3a: Preferential sputtering in depth profiling of a Ta/Si (7.5/10.5 nm) multiplayer, sputter profiles with 1 keV Ar^+ ions at 81 deg. incidence angle. MRI parameters are : w= 2.6 nm, σ = 1.1 nm, λ = 0.4 nm, sputtering rate ratio r(Si/Ta) = 3.5. From [13].

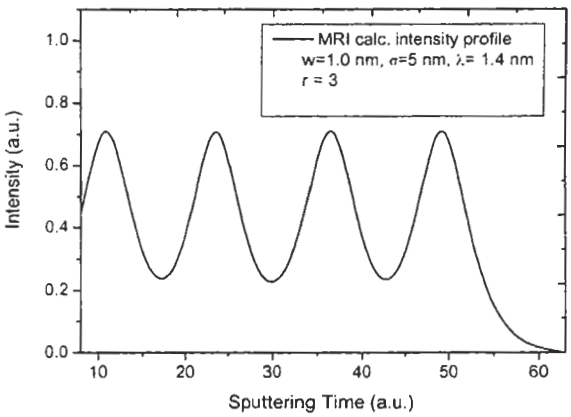

Fig. 3b: MRI calculation for preponderant roughness showing symmetric peaks in contrast to Fig. 3a.

6. Changes of parameters in interface sputtering

Sputtering through interfaces is obviously a case where matrix effects are most pronounced. Therefore interface profiling is particularly difficult to quantify in SIMS, whereas in AES matrix effects are generally much smaller, but they still may lead to errors in quantification of the order of 30%. Changes of the relative elemental sensitivities, due to backscattering as well as

to roughness effects, can be corrected before applying the MRI model. However, changes of the MRI parameters (σ, w, λ) when sputtering through interfaces have to be taken into account in the model itself.

6.1 Change of σ: roughness and diffusion

One of the great achievements to reduce or practically eliminate sputtering induced roughness in thin films was the introduction of sample rotation during profiling by A. Zalar in 1985. However, there is still some roughness left, remaining from the film growth and/or caused by the statistical nature of the sputtering process. Changing roughness when sputtering through an interface can be encountered, for example, when sputtering induced second phases are evolving. Except for such special cases, roughness stays constant when using sample rotation and/or high incidence angle of the ions. Roughness within the MRI model is described by a Gaussian function. Because in (ideal) diffusion, each delta layer is also broadened by a Gaussian function. The standard deviation of that Gaussian, σ_{Diff}, is simply given by the mean diffusion length, $(2Dt)^{1/2}$. The diffusion constant is then given by [5]:

$$D = \frac{\sigma_{Diff}^2}{2t} = \frac{\sigma_T^2 - \sigma_0^2}{2t} \qquad (2)$$

where t is the annealing time, σ_T and σ_0 are the MRI roughness parameters after and before annealing, respectively. An example was shown in [5]. A triple layer of Ge in Si was annealed for 30 min. at 650 and 700 °C. The MRI fit of the measured Ge profile of the sample before and after annealing gave the MRI parameters σ_0 = 0.8 nm and σ_T (700C) = 1.7 nm. With eq. (2) the diffusion constant was determined to be D = 6.3 x 10^{-22} m^2/s. Annealing at several temperatures enables the determination of the activation energy and the pre-exponential term as usual. It should be emphasized, that quantitative evaluation of sputtering profiles by the MRI model with a very high precision of about ± 0.1 nm allows the determination of diffusion constants as low as 10^{-22} m^2/s for relatively short annealing times (30 min.). It also allows the determination of local diffusion coefficients with a resolution of typically several nanometers.

6.2 Change of w: profiling through interfaces

Because the mixing length depends on the material, it will generally change when sputtering through an interface. In general, the change of w is neglected and an average mixing length (about the average ion range taken from TRIM code calculations) is assumed for the calculation [15].

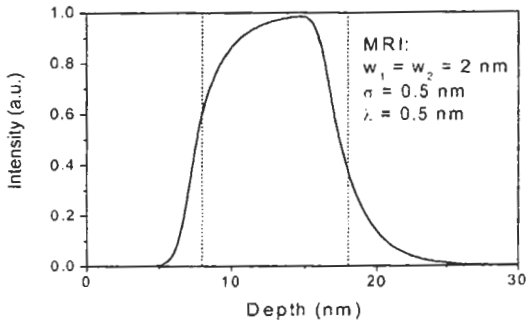

Fig. 4a: MRI profile calculation of a 10 nm thick layer with the shown parameters with preponderant, constant mixing parameter w.

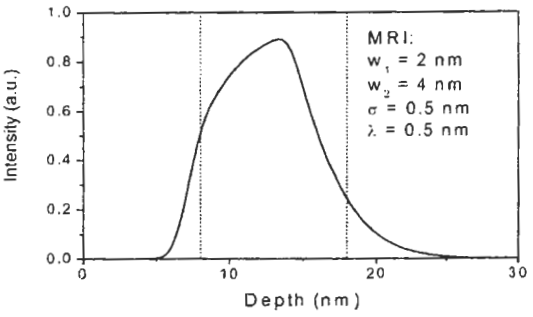

Fig. 4b: MRI profile calculation of the layer in fig.4 a with a different mixing length w in the layer (w_2) and in the matrix (w_1).

Because this is only an approximate value, the final w is found by trial and error in the vicinity of that value. A better approximation appears to be to consider the change of the parameter w through the interface A/B (of components A and B) by introducing a linear dependence on the composition, for example $w = X_A w_A + X_B w_B$. The interface profiles are given for $w_1 = w_2$ = 2 nm in Fig. 4a, and for w_1= 2 nm and w_2=4 nm in Fig. 4b. Although

the simplification of an average w seems to be justified in most cases, it is recognized, e.g. by comparing Fig. 4 b with Fig. 3 a, that there is a certain similarity of the typical shape of a multilayer profile in the MRI model for preferential sputtering and for changing of w at the interfaces.

6.3 Change of λ: AES depth profiling through interfaces

In contrast to SIMS, where the information depth is practically constant and of the order of 1-2 monolayers, the change of the electron escape depth with composition is obvious in AES depth profiling. Again we may approximate that dependence by assuming a linear relation between the attenuation cross sections (that are given by $1/\lambda$) and composition, i.e.[16]:

$$1/\lambda = X_A/\lambda_A + X_B/\lambda_B \qquad (3)$$

Introducing equ. (3) in the MRI model shows the influence on the profile. In general, the profile shape is not dramatically changed. Recently, by using reflection electron energy loss spectroscopy (REELS) depth profiling to directly determine the change of the inelastic mean free path when sputtering through an Fe/Si interface, a nearly linear dependence from λ'_{Fe} = 1.8 nm to λ'_{Si} = 2.4 nm was observed [17].

7. Conclusions

Recent progress in quantitative sputter depth profiling using the MRI model was achieved by specific applications in specific fields. For example, the symmetric Gaussian component of the MRI depth resolution function can be used as a quantitative, accurate measure of diffusion in thin films. For low roughness, the strong asymmetry of the depth resolution function in SIMS enables quantitative prediction of the results of backside sputter profiling. The dependence of the apparent shift of the measured profile towards the surface on the electron escape depth in AES depth opens an intrinsic way of estimating the sputtered depth from simultaneous measurements of low and high energy Auger peaks of the same element by their different shift. Nonlinear relationships between intensity and concentration as well as between sputtering time and sputtered depth (i.e., preferential sputtering) can be taken into account by slight extensions of the MRI model. Further modifications by introducing a linear dependence of the mixing length and of the attenuation of the Auger electrons on composition in a binary system help to attain a new stage of improved accuracy for interfacial depth profiling.

References

[1] S. Hofmann, Surf. Interface Anal. 30, 228 (2000).
[2] S. Hofmann, Thin Solid Films 398-399, 336 (2001).
[3] S. Hofmann and K.Yoshihara, J. Surf. Anal. 5, 40 (1999).
[4] T. Kitada, T. Harada and S. Tanuma, J. Vac. Soc. Japan, 38, 252 (1995).
[5] V. Kesler and S. Hofmann, J. Surf. Anal. 9, 428 (2002).
[6] S. Hofmann, Surf. Interface Anal. 27, 825 (1999).
[7] K. L. Yeo, A.T.S. Wee, R. Liu, C.M. Ng and A. See, Surf. Interface Anal. 33. 373 (2002).
[8] S. Hofmann, Surf. Interface Anal. 20, 673 (1994).
[9] S. Hofmann, Vacuum 48, 607 (1997).
[10] S. Hofmann, Surf. Interface Anal., to be publ.
[11] S. Hofmann, J. Surf. Anal., to be publ. (Sekine issue)
[12] S. Hofmann, A. Rar, D. W. Moon, and K. Yoshihara, J. Vac. Sci. Technol. A 19, 1111 (2001).
[13] S. Hofmann and J. Y. Wang, J. Surf. Anal. 9, 306 (2002).
[14] S. Hofmann and A. Zalar, Thin Solid Films 60, 201 (1979).
[15] S. Hofmann and V. Kesler, Surf. Interface Anal. 33, 461 (2002).
[16] M. Menyhard, Surf. Interface Anal. 26, 1001 (1998).
[17] P. Prieto, S.Hofmann, E. Elizalde and J.M. Sanz, Poster at QSA 13, to be published in SIA.